Supporting Information

Chen *et al.* 10.1073/pnas.0804918105

SI Methods

Electrophysiology. Coronal slices (300 μm) containing primary somatosensory cortex were prepared from mice age P17–P24. Slices were stored for at least 1 h at 37°C in oxygenated artificial cerebrospinal fluid (ACSF) with final concentrations of 126 mM NaCl, 3 mM KCl, 2 mM $MgSO_4$, 1 mM NaH_2PO_4, 25 mM $NaHCO_3$, 2 mM $CaCl_2$, and 10 mM dextrose and were transferred to a thermoregulated recording chamber and perfused continuously with oxygenated ACSF containing synaptic blockers 2-amino-5-phosphonovaleric acid (APV; 50 μM), 6,7-dinitroquinoxaline-2,3-dione (DNQX; 20 μM), and bicuculine (20 μM). Visually guided whole-cell patch–clamp recordings from pyramidal neurons in lower layer 5 were made by using an AxoPatch 200B amplifier (Axon Instruments). Recording pipettes of 3- to 5-MΩ resistance contained internal solution with final concentrations of 20 mM KCl, 100 mM potassium gluconate, 10 mM Hepes, 4 mM Mg-ATP, 0.3 mM Na-GTP, 10 mM sodium phosphocreatine, 0.1% biocytin. Data were filtered at 10 kHz and collected on a Dell computer using custom software running on Igor Pro (WaveMetrics). Analyses of recorded responses were performed in Igor and Matlab (Mathworks). To measure spike frequency adaptation, we analyzed responses recorded at two times the threshold current. The adaptation ratio is defined as the ratio of the third interspike interval to the last interspike interval and is reported as mean ± SEM. Statistics were calculated from Student's *t* test or from Hartigan's statistic for unimodality by using a bootstrap sample size of 10,000. Cells were filled with biocytin through the recording pipette and fixed overnight in a buffered solution containing 4% paraformaldehyde. To visualize labeled cells, sections were reacted with the ABC Elite kit (Vector Laboratories) and 3–3′-diaminobenzidine (DAB).

Dendritic Analysis. For dendritic analysis, the distance from the tip of each terminal branch to the pial surface was measured for each biocytin-filled neuron. The distances of all of the terminal branches on a signal neuron were averaged and compared. In addition, the number of branches in each tuft was counted for each neuron. ANOVAs (StatView version 5.0.1; SAS) were performed to compare both the distances of apical dendrites from the pial surface and the numbers of branches in three different groups: adapting neurons, nonadapting neurons, and neurons in *Fezf2*$^{-/-}$ mutant brains.

Cloning of *Fezf2* and *Ctip2* into pCA-pcDNA Expression Vectors. The *pCA-pcDNA3.1* vector was generated by S. Wilson in the McConnell laboratory and kindly provided for these experiments. This vector utilizes the cytomegalovirus enhancer fused to the chick β-actin promoter to drive gene expression. The primers gtggtggaattcgccgccgccatggccagctcagcttccctggagaccatggtg and tgctggatatcagctctgaactgtcctggctaggtcctttgctgag were used to amplify the *Fezf2* cDNA. The primers gtggtggaattcgccgccgccatggccatgtcccgccgcaaacagggcaacccgcagcac and tgctggatatcagctcctctcagcctgctcgattttgacatcat were used to amplify *Ctip2* cDNA. The plasmid *pEF1αZfp312iresGFP* was a gift from Nenad Sestan at Yale University.

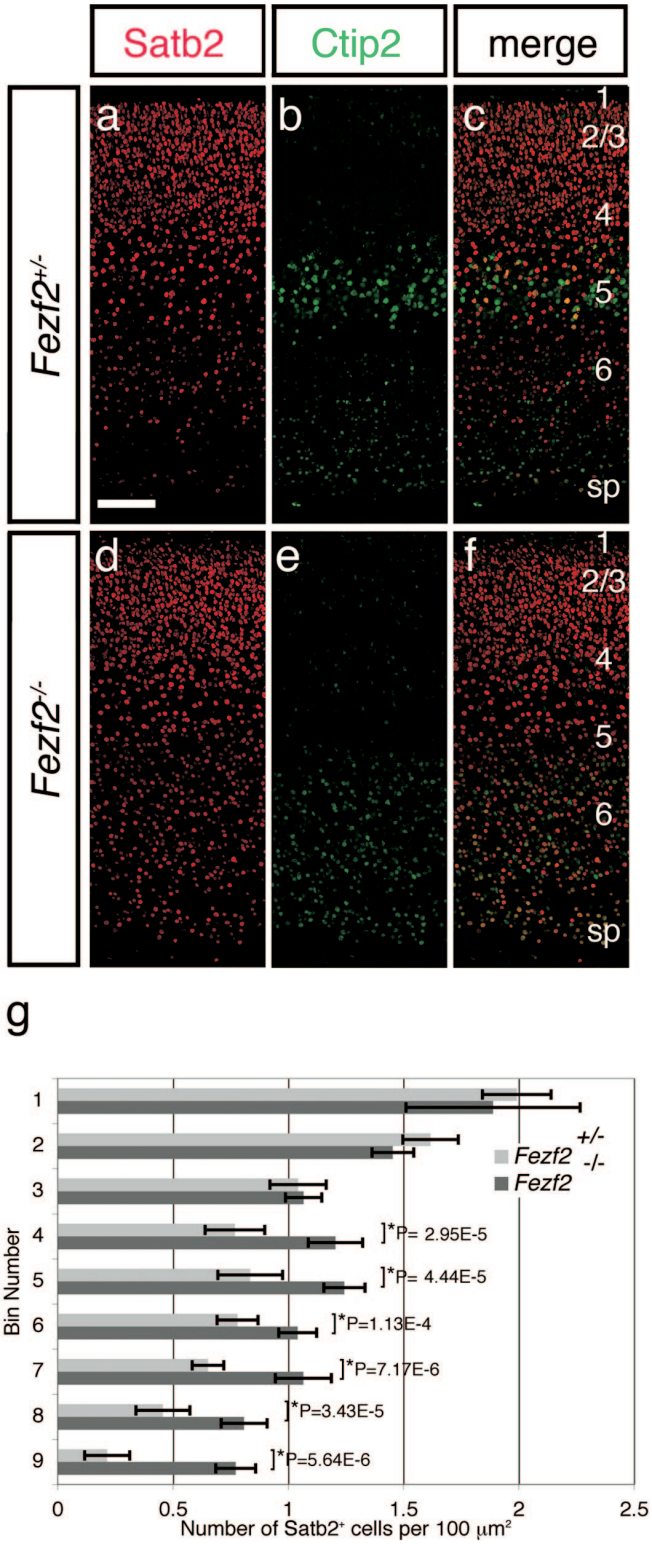

Fig. S1. The deep layers in anterior–medial cortical regions of *Fezf2*$^{-/-}$ mice show increased Satb2 expression. Anatomically matched sections from anterior–medial regions of control mice (*a–c*) and *Fezf2*$^{-/-}$ (*d–f*) mice at P4 were immunostained for Ctip2 (green) and Satb2 (red). Satb2 expression was increased in the deep layers of *Fezf2* mutants. (Scale bar, 100 μm.) (*g*) Histogram comparing the densities of Satb2^{+} neurons in mutant vs. control brains. Statistically significant changes were observed in deeper but not more superficial positions (*, $P < 0.01$; Student's *t* test). Cells that coexpress Ctip2 and Satb2 in layer 5 appeared more prominent in anterior–medial cortex compared with posterior regions (Fig. 3) and compared with the reported figure of <5% coexpression [Alcamo EA, *et al*. (2008) Satb2 regulates callosal projection neuron identity in the developing cerebral cortex. *Neuron* 57:364–377].

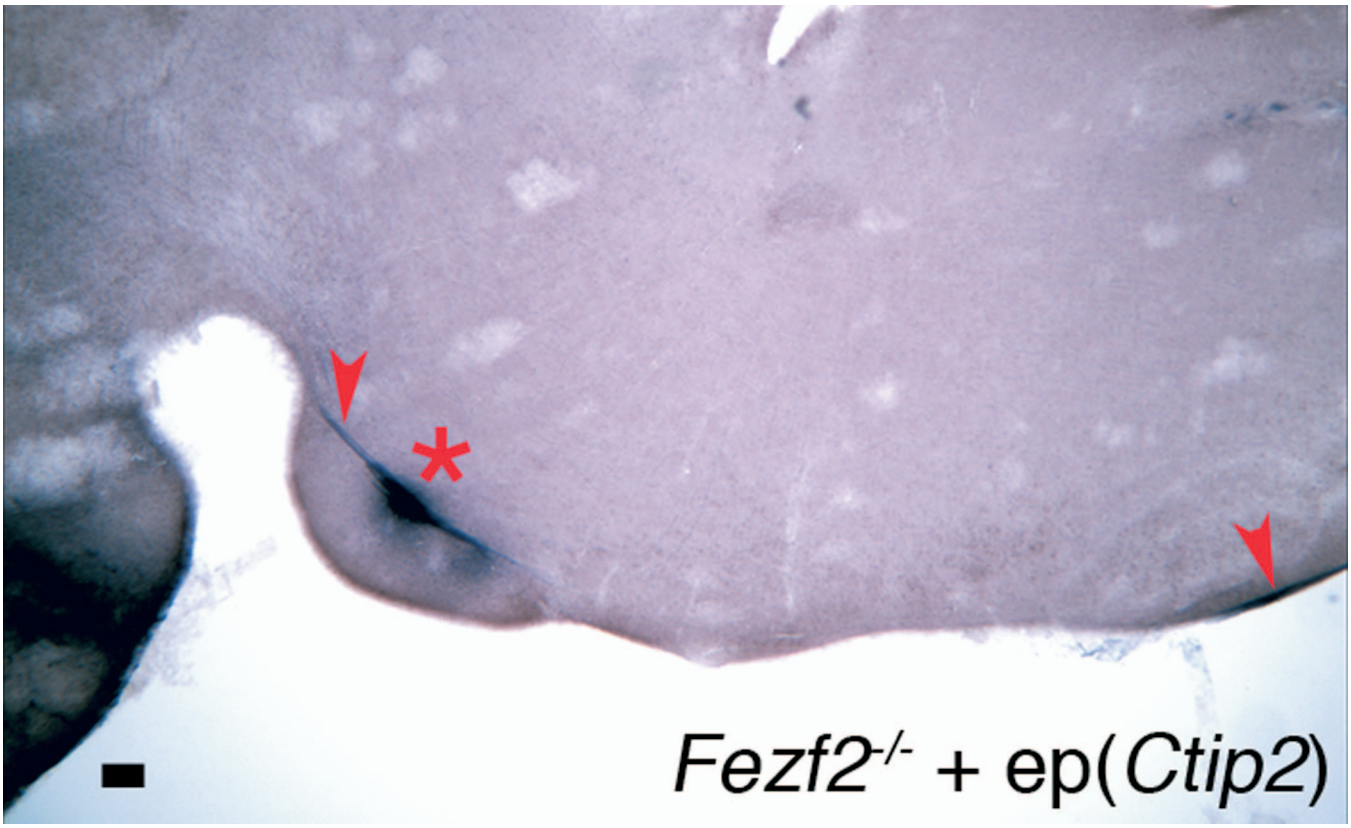

Fig. S2. PLAP-labeled axons in the pyramidal tract of P2 mice branched in the pons after *Ctip2* cDNA was electroporated into the cortical neurons of the *Fezf2*$^{-/-}$ mice at E13.5. The red arrows point to the pyramidal tract, and the star labels axon branching in the pons. (Scale bar, 100 μm.)

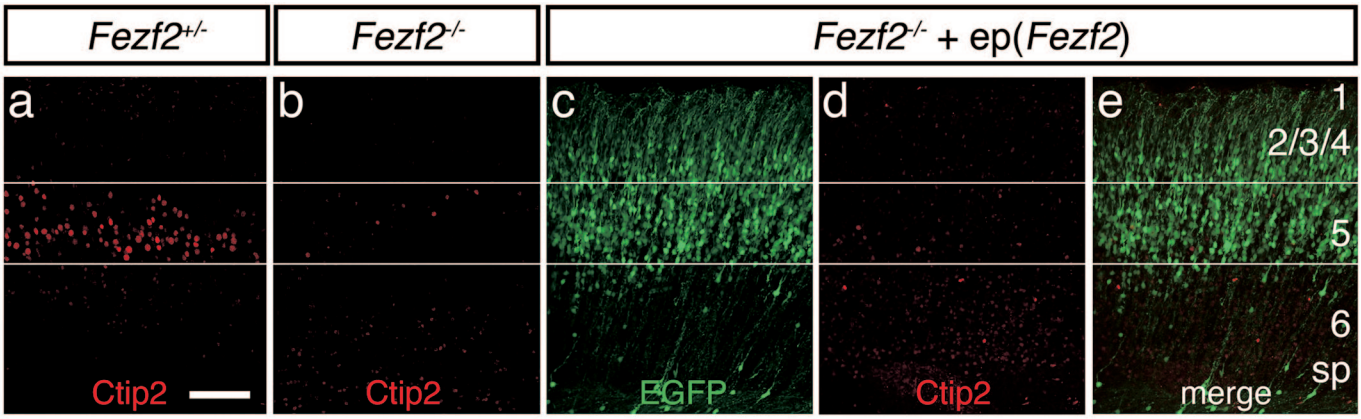

Fig. S3. Electroporation of *pCA-Fezf2* cDNA into the *Fezf2*$^{-/-}$ cortex at E13.5 does not restore Ctip2 expression in deep-layer neurons at P0. (*a*) Ctip2 (red) is expressed in layers 5 and 6 of *Fezf2*$^{+/-}$ mice at P0. (*b*) Ctip2 expression (red) is severely disrupted in the deep layers of *Fezf2* mutants. (*c*–*e*) Coelectroporation of *pCA-EGFP* and *pCA-Fezf2* expression constructs into *Fezf2* mutant embryos at E13.5. EGFP expression (green) reveals that most electroporated cells migrate to layer 5 (*c*), but Ctip2 protein (red) was not detected in electroporated cells (*d* and *e*). White lines mark the boundaries of layer 5 in all panels. ep, electroporation (expression construct). (Scale bar, 100 μm.)

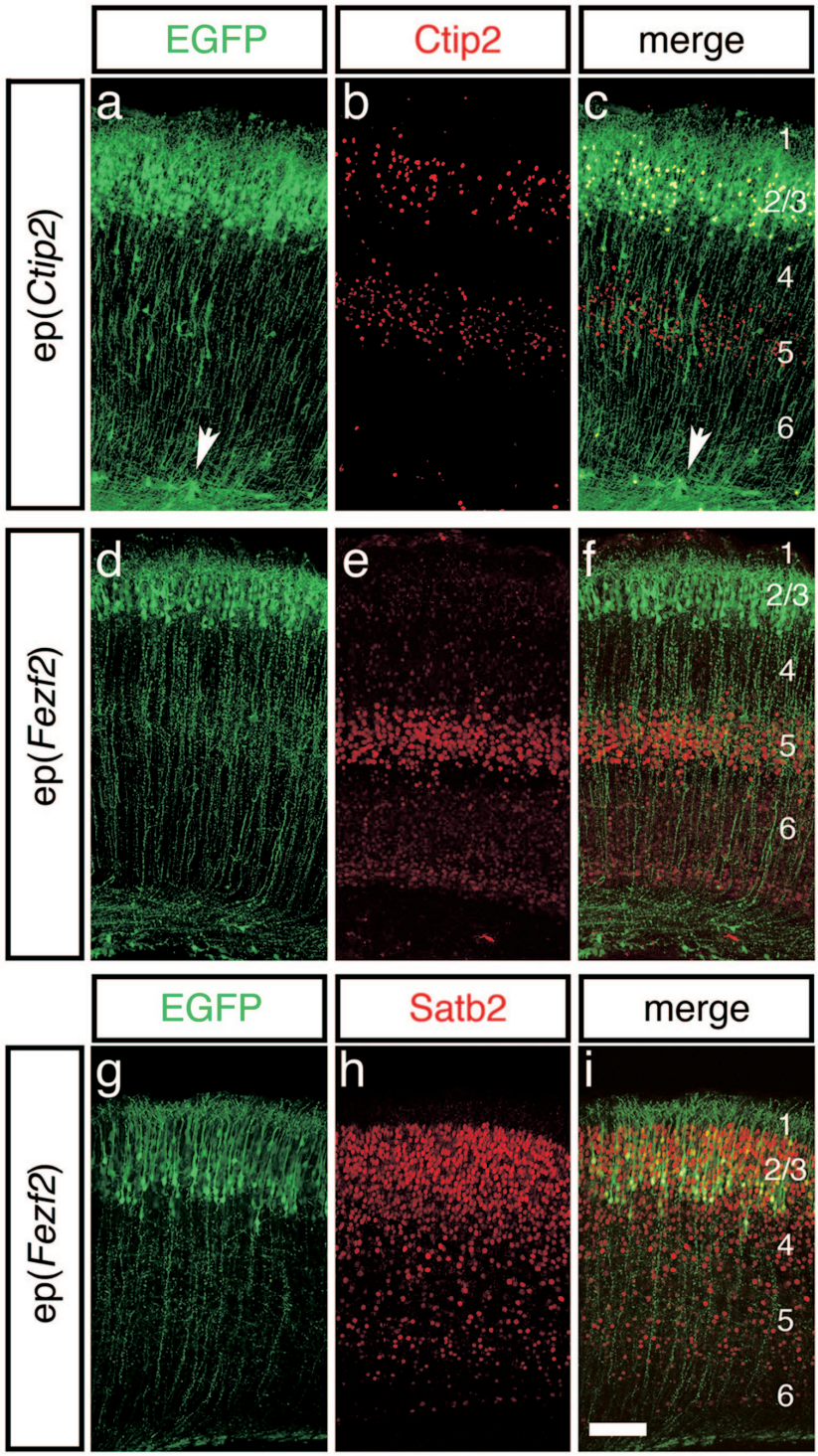

Fig. S4. Ectopic expression of *Fezf2* cDNA at E15.5 is not sufficient to induce the expression of Ctip2 in upper-layer neurons at P5. (*a*–*c*) Coelectroporation of *pCA-Ctip2* and *pCA-EGFP* into layer 2/3 neurons results in the expression of Ctip2 protein (*b* and *c*, red) in electroporated layer 2/3 neurons (*a* and *c*, green). Ctip2 immunoreactivity is also visible in layer 5, where it is normally expressed at high levels. Some electroporated cells remained in the white matter (*a* and *c*, arrows). (*d*–*f*) Electroporation of *pCA-Fezf2* and *pCA-EGFP* into layer 2/3 neurons fails to induce the expression of Ctip2 protein (red) in electroporated upper-layer neurons (green). Ctip2 immunoreactivity is present in wild-type layer 5 neurons. (*g*–*i*) Ectopic expression of *pCA-Fezf2* and *pCA-EGFP* in layer 2/3 neurons (green) does not repress Satb2 expression (red), as indicated by the presence of numerous double-labeled cells (*i*). ep, electroporation (expression construct). (Scale bar, 100 μm.)

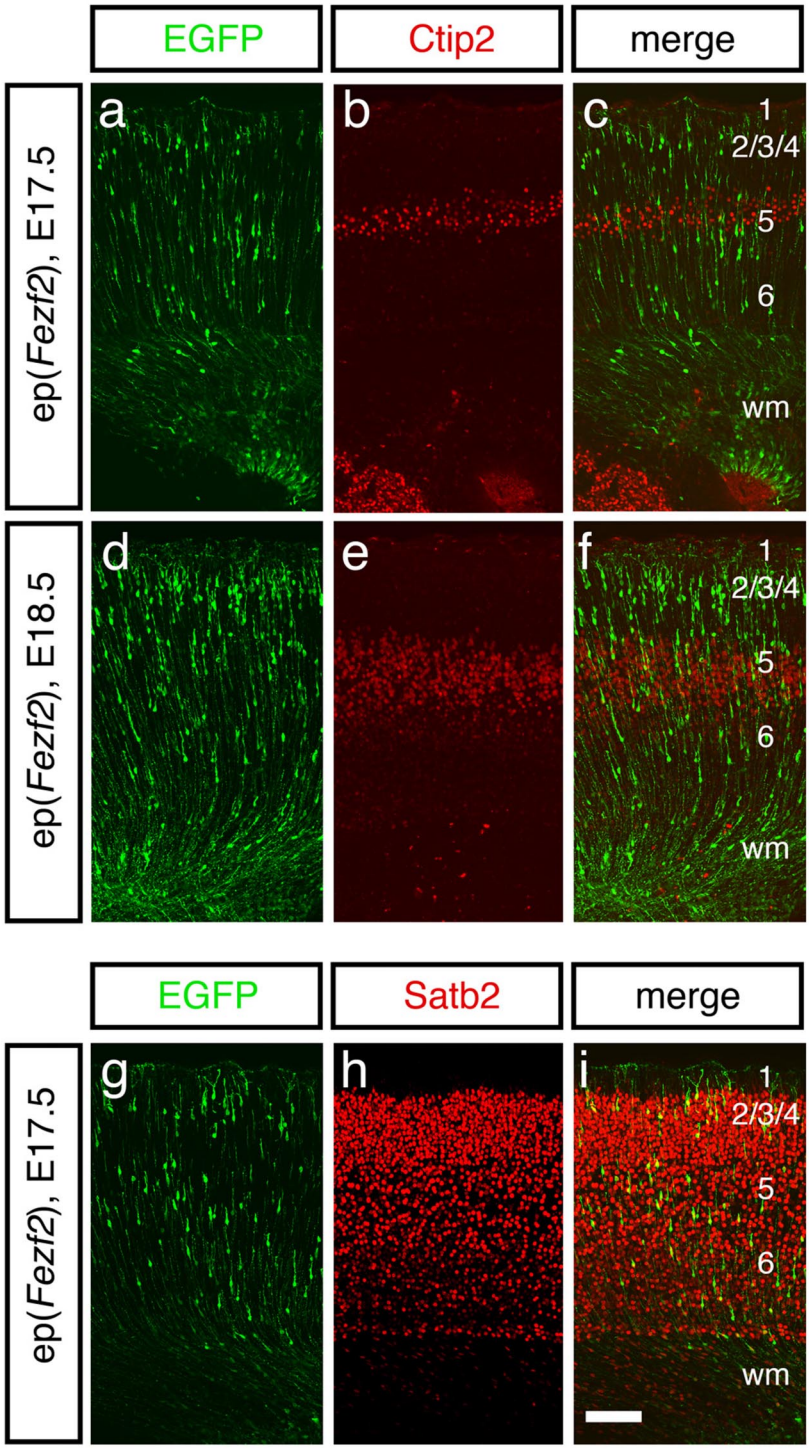

Fig. S5. Ectopic expression of *Fezf2* cDNA at E15.5 is not sufficient to induce the expression of Ctip2 in migrating upper-layer neurons. (*a*–*c*) Coelectroporation of *pCA-Fezf2* and *pCA-EGFP* at E15.5 does not induce Ctip2 expression (*b* and *c*, red) in electroporated migrating neurons (*a* and *c*, green) at E17.5. (*d*–*f*) Electroporation of *pCA-Fezf2* and *pCA-EGFP* at E15.5 fails to induce Ctip2 expression (red) in electroporated neurons (green) at E18.5. (*g*–*i*) Ectopic expression of *pCA-Fezf2* and *pCA-EGFP* in migrating layer 2/3 neurons (green) does not repress Satb2 expression (red) at E17.5. ep, electroporation (expression construct). (Scale bar, 100 μm.)

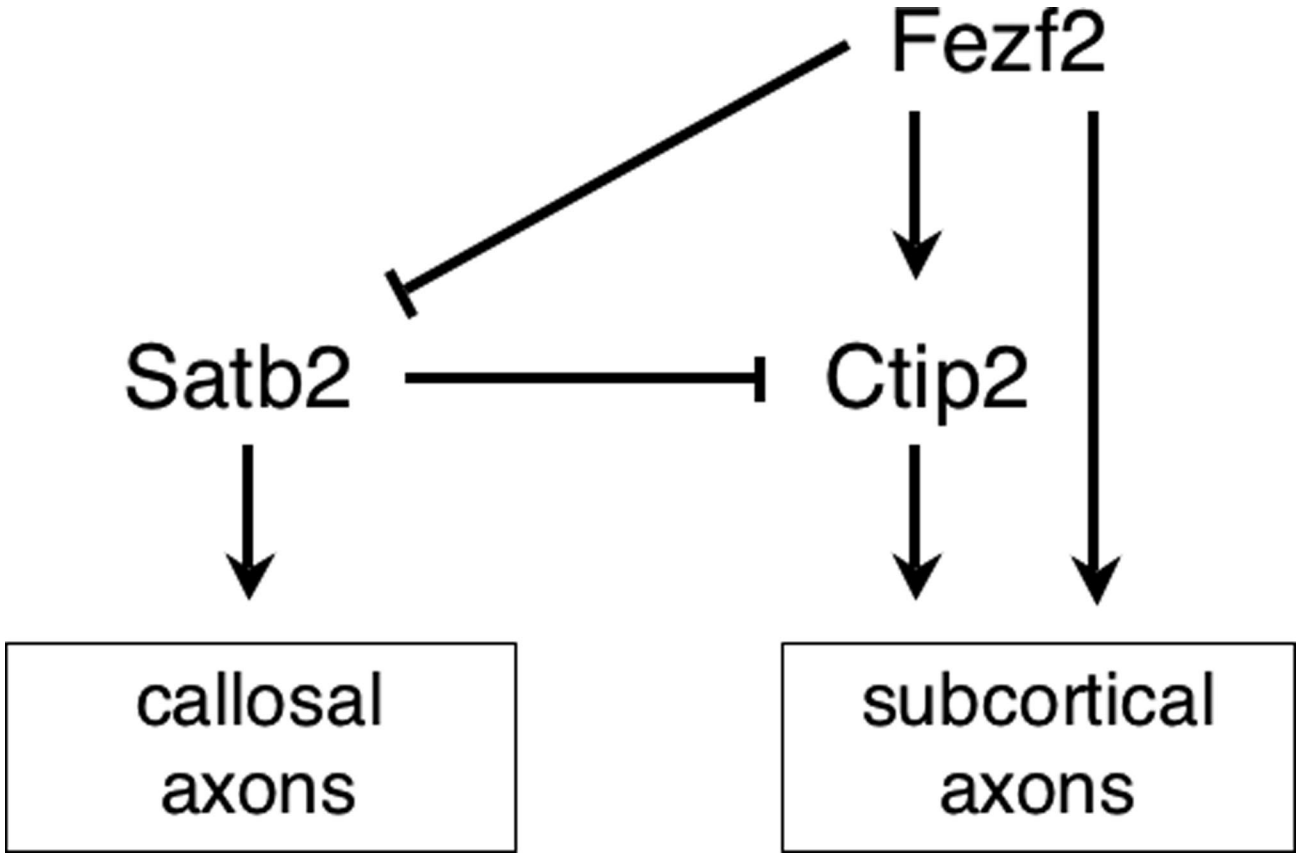

Fig. S6. Diagram showing the relationship among Fezf2, Ctip2, and Satb2.